Supporting Information for "Experimental Methods and Imaging for Enzymatically Induced Calcite Precipitation in a micro-fluidic cell"

Felix Weinhardt[1], Holger Class[1], Samaneh Vahid Dastjerdi[2], Nikolaos

Karadimitriou[2], Dongwon Lee[2], Holger Steeb[2,3]

[1]Department of Hydromechanics and Modelling of Hydrosystems, University of Stuttgart, Pfaffenwaldring 61, 70569 Stuttgart,

Germany

[2]Institute of Applied Mechanics, University of Stuttgart,Pfaffenwaldring 7, 70569 Stuttgart, Germany

[3]SC SimTech, University of Stuttgart,Pfaffenwaldring 7, 70569 Stuttgart, Germany

Contents of this file Figures S1 to S4

Introduction

This supporting information provides two sketches of the experimental set-ups: one of the open and modular XRCT device (Figure S1) and another one of the custom made optical microscope, including the stage of the experimental set-up (Figure S2). Moreover, two flow charts describing the image processing steps are given: One visualizes the steps for the images taken by optical microscopy (Figure S3) and the other one for the XRCT dataset (Figure S5). Furthermore a comprehensive description of the image processing of the XRCT-dataset is given below.

August 6, 2020, 2:08pm

Description of open and modular XRCT device

The scan was performed in open and modular XRCT device which was set-up during the last years. It is based on an open micro-focus tube with a tungsten transmission target (FineTec Force 180.01C TT, FineTec Technologies GmbH, Germany). The detector (Shad-o-Box 6K HS, Teledyne DALSA Inc., Waterloo, Ontario, Canada) has an active area of 146×114 mm^2 with a pixel size of 49.5 μm which results in images of the size of 2940×2304 pixels. The Shad-O-Box detector has a CsI-scintillator and the image output of the detector is realized via GigE interfaces using LAN connections to the computer. The cone-beam scanning process was carried out without any physical filtering. A schematic illustration of the scanning device can be seen in S1. The voltage, the current, and the exposure time were set to 80 kV, 100 μA and 3000 ms respectively. The scan consists of 1800 projections (5 rotation fragments per degree). In order to minimize ring artefacts, the output of 5 slightly shifted projections are averaged at each (rotational) position. Therefore, the detector was moved slightly to the left, right, up, and down. The resolution was set to 4.25 μm/px to obtain 20 voxels in the depth of the porous domain. Given the total number of 9005 images, the scanning has taken 15 hours and 46 minutes. Reconstruction of the 3D volume is performed by the software tool Octopus Reconstruction (Version 8.9.4-64 bit). A schematic illustration of the set-up is shown in Figure S1.
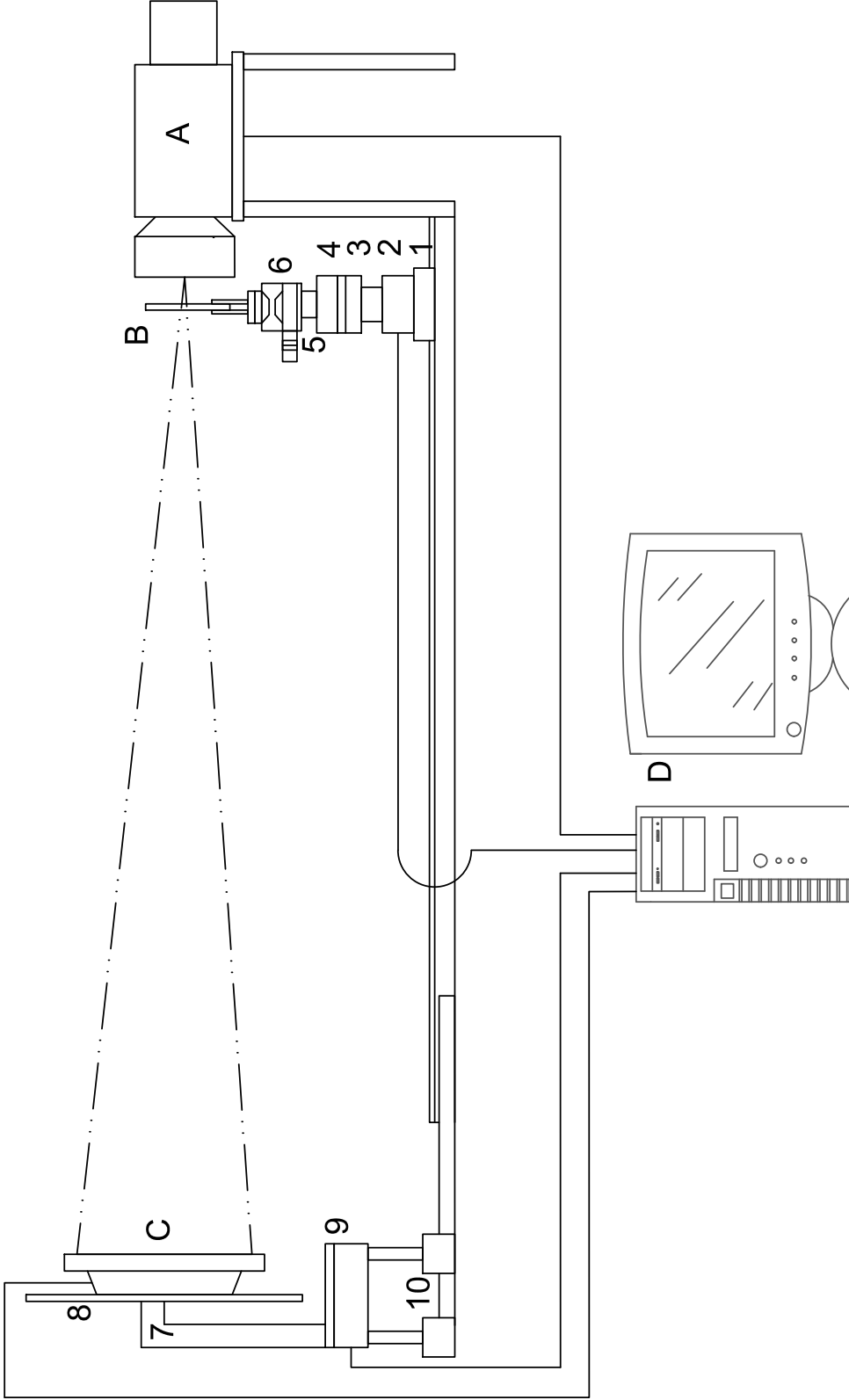
Figure S1. Components of the open and modular XRCT device: (A) shows the micro-focus source. (B) is the cell under XRCT investigation. Further, various (motorized) stepper and DC motor-based stages (1-6) including the rotational stage (4) and various translation stages (1-3) and the x-y-stages (5-6) for sample positioning are shown. (C) is the detector and the stages (8-10) are used for detector movements incl. ring artefact minimization. The stages, the detector and the source are computer-controlled (D) with in-house tools
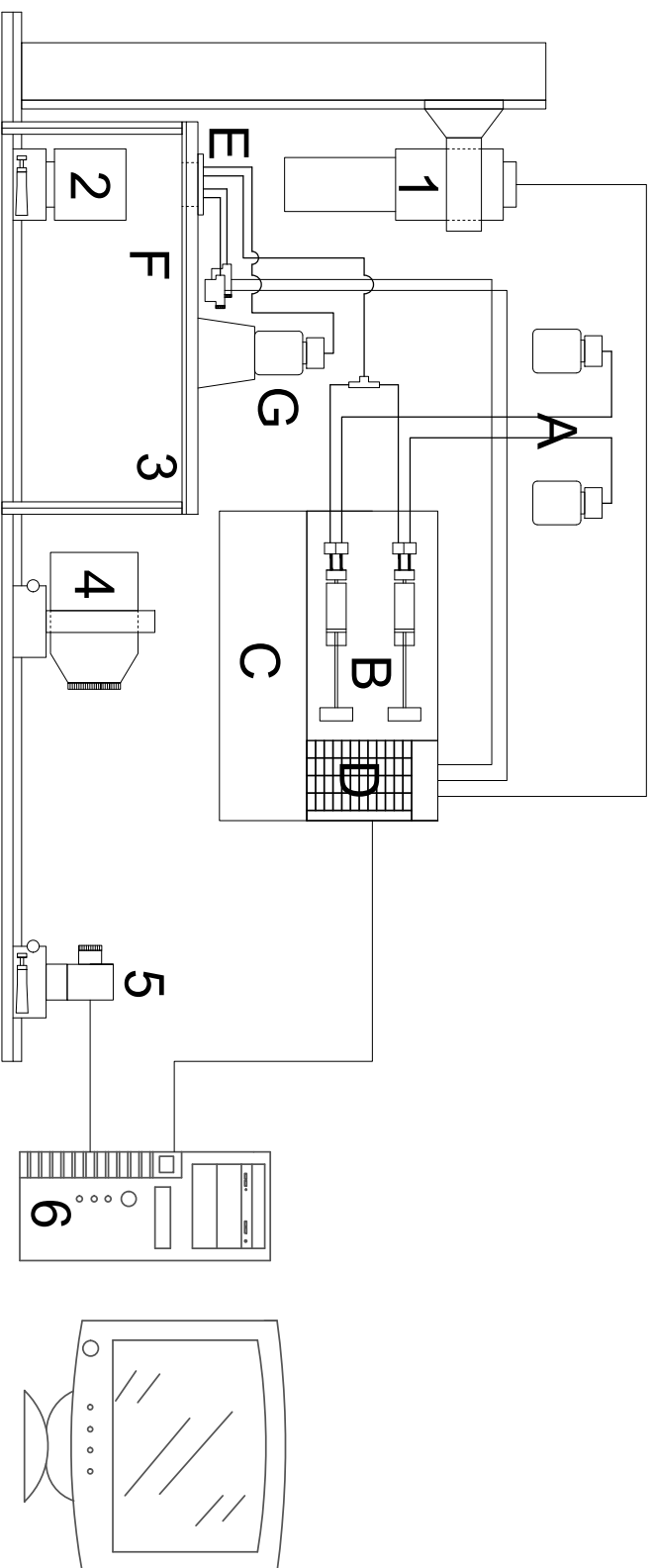
:

Figure S2. 1-6: Parts of the open microscope; 1: Light source (1W LED light source emitting at 590 nm mounted on Canon objective lens with F 3.2/135 mm); 2: Prism (Edmund Optics with dimension of 50 mm x 50 mm); 3: Stage for the micro-fluidic cell; 4: Lens (Sigma 135 mm F1.8 DG HSM telephoto lens); 5: Camera (Allied Vision GigE GC-D-2450 camera with a 5 Mpx sensor); 6: Computer. A-G: Parts of the micro-fluidic system: A: Reservoir (filled with water for stage a and c or filled with the two reactive solutions for stage b; B: Syringe pumps (CETONI neMESYS 100N) C: CETONI base module; D: CETONI I/O module 16 bit; E: micro-fluidic cell; F: Pressure sensors (Elveflow MPS03, range 0 − 70 mbar); G: Outlet reservoir

Detailed description of image processing for the XRCT-dataset

In Figure S5 various stages of the image processing, carried out to extract the desired data out of the reconstructed images from the XRCT. Embedded in the process, which is already explained in the paper, there are some measures, taken to tackle the existence of a second phase around some of the crystals. In the following, the mentioned processes are described.

After the 3D dataset was cutted and aligned, it was read into Matlab R2019b (The Mathworks, Inc.) as 20 images, each representing one layer in the depth of the channel. Then images were segmented using the "Max Entropy Thresholding" method. This method gave us the precipitates along with parts of the channel wall. So, there was a need for a mask to remove the non-relevant voxels. By adding up all the segmented images together, and cleaning the resulting image manually, a mask was prepared. This was done to avoid cleaning all of the images one by one. This mask was multiplied by all of the images to remove the noise but keep the crystals untouched. In another attempt, the same procedure was carried out with one difference: The segmentation was done by multithresholding, Otsu's method. This gave us the crystals which has some other phase around them, in two parts. The reason why the multithresholding, Otsu's method is not used for all of the crystals, is that a layer around the crystals have the same gray value as in the second phase and is categorized as the second phase. To sum it up, 4 of the crystals where a second phase is observed in the XRCT were segmented with multithresholding, Otsu method and the rest with maximum entropy. There was an issue with the multi-thresholding method, which needed to be addressed: Due the gray value distribution on the first and last slide, this method, classifies all of the voxels on the top and at the bottom of the channel as the second phase. That led for the crystals, with the second phase around them to be connected to nowhere, which is physically not possible. For this reason a closer look at the not processed XRCT images

raw image: Gray scale image of the initial state

Filtering and segmentation: (*imdiffusefilt*) (*imbinarize*)

flood-fill and morphological operation: (*imfill*) (*imclose*)

geometrical operation: crop and rotate image (*imrotate*)

binary mask: 1: porous domain 0: outside of porous domain

raw images: Gray scale image at different timestamps

Image registration: Register to initial image (*imregister*)

geometrical operation: crop (*imrotate*) element wise multiplication with mask

Filtering and segmentation: (*imdiffusefilt*) (*imbinarize*)

Processed images: binary image 1: void space 0: solid

Processed binary images

estimateion of porosity change

Calculate 2D porosity: mean (binary image)

Identify inivival crystal aggregates and their projection area: (*regionprops*)

3D shape assumption

cylindrical

Semi-sperical

spherical

spheroidal

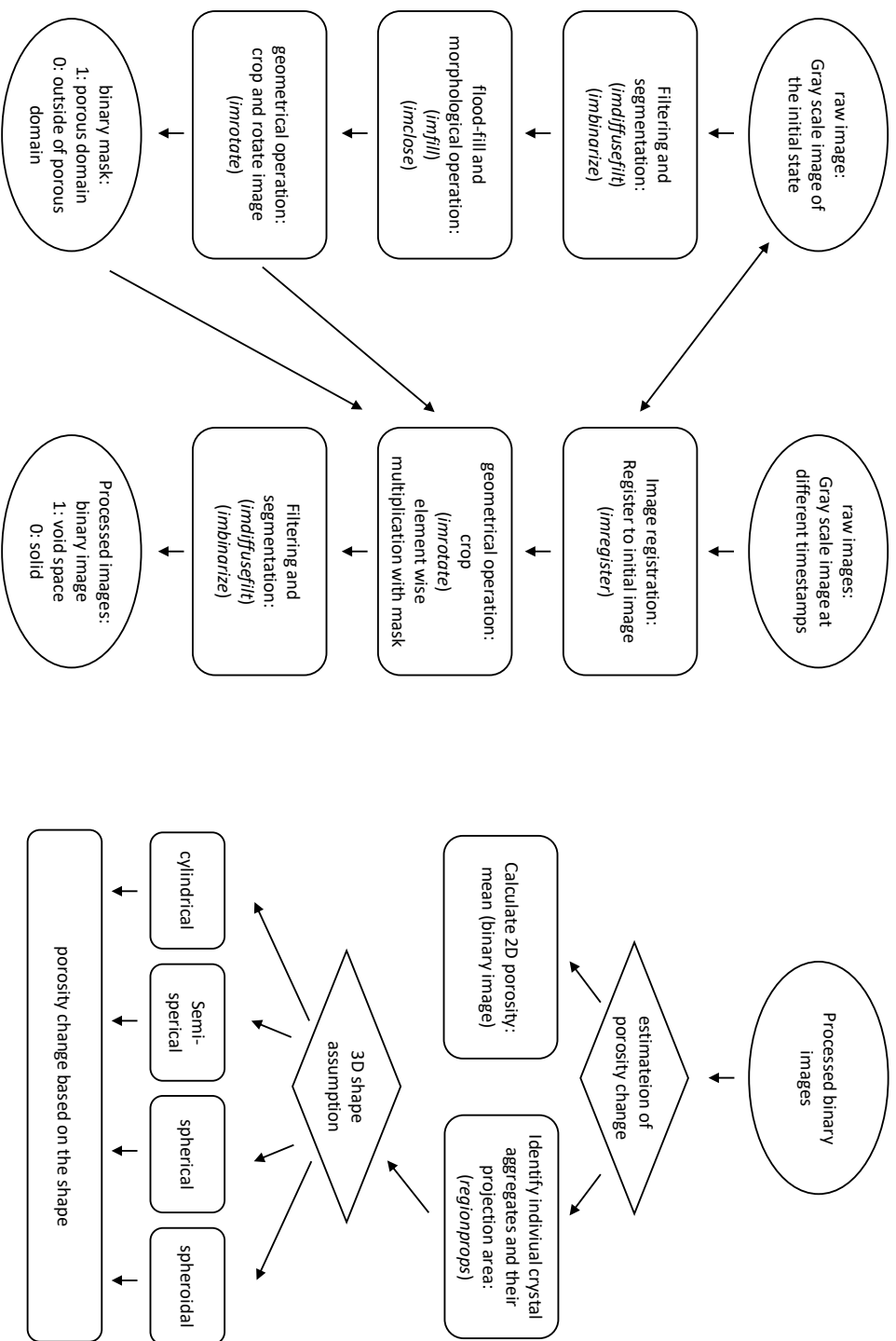porosity change based on the shape

Figure S3. Flow chart of image processing for optical microscopy images. Left: Creating the mask from the initial image; mid: segmenting the gray scale images; right: further processing of the segmented images in order to calculate the pore space ration of the precipitates
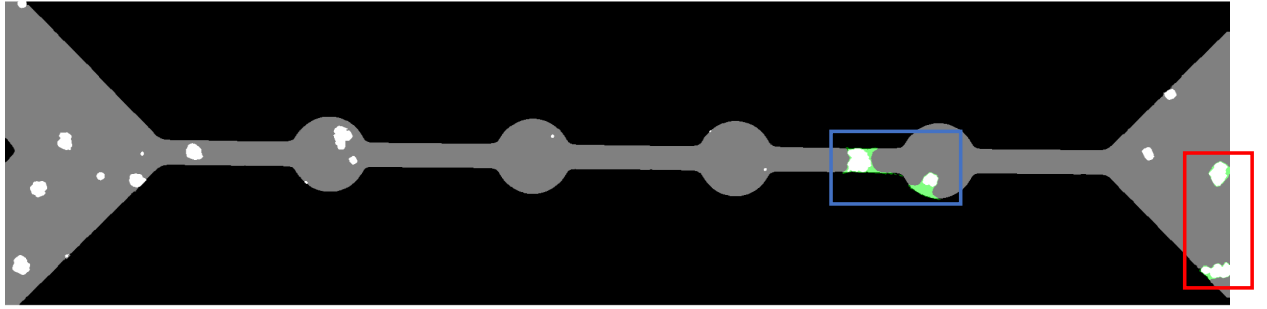
Figure S4. Second phase allocation in the precipitated cell

was required to have a dataset resembling the XRCT as good as possible. The XRCT-images guided us to the following:

The four crystals marked with the blue and red box in S4 are the crystals with the second phase around them. However they are not treated similarly and that is because a bow form is observed in the channel, meaning that the channel is not completely horizontal. The middle of the channel is roughly 2 voxels higher than the two ends. The 20 slides which are defining the channel depth are chosen with reference to the middle of the cell. For the two crystals which are in the middle of the cell and are not affected by the hypothetically physically bow form of the channel (marked with the blue box), the following is done: The last layer of the crystal in depth is defined as the layer below it. It means in the final dataset, the 1st and 20th layer of these two crystals is the same as the 2nd and 19th respectively. For the other two (marked with red box) which are placed closed to the edges, other measures are carried out. In them the crystals are shifted three voxels up and the first three layers are defined as the fourth one. It means that the 1st, 2nd and 3rd layers of the named crystal, resemble the 4th one. Finally the segmented volume of the all of the crystals were put together as the final dataset and used for the investigations.
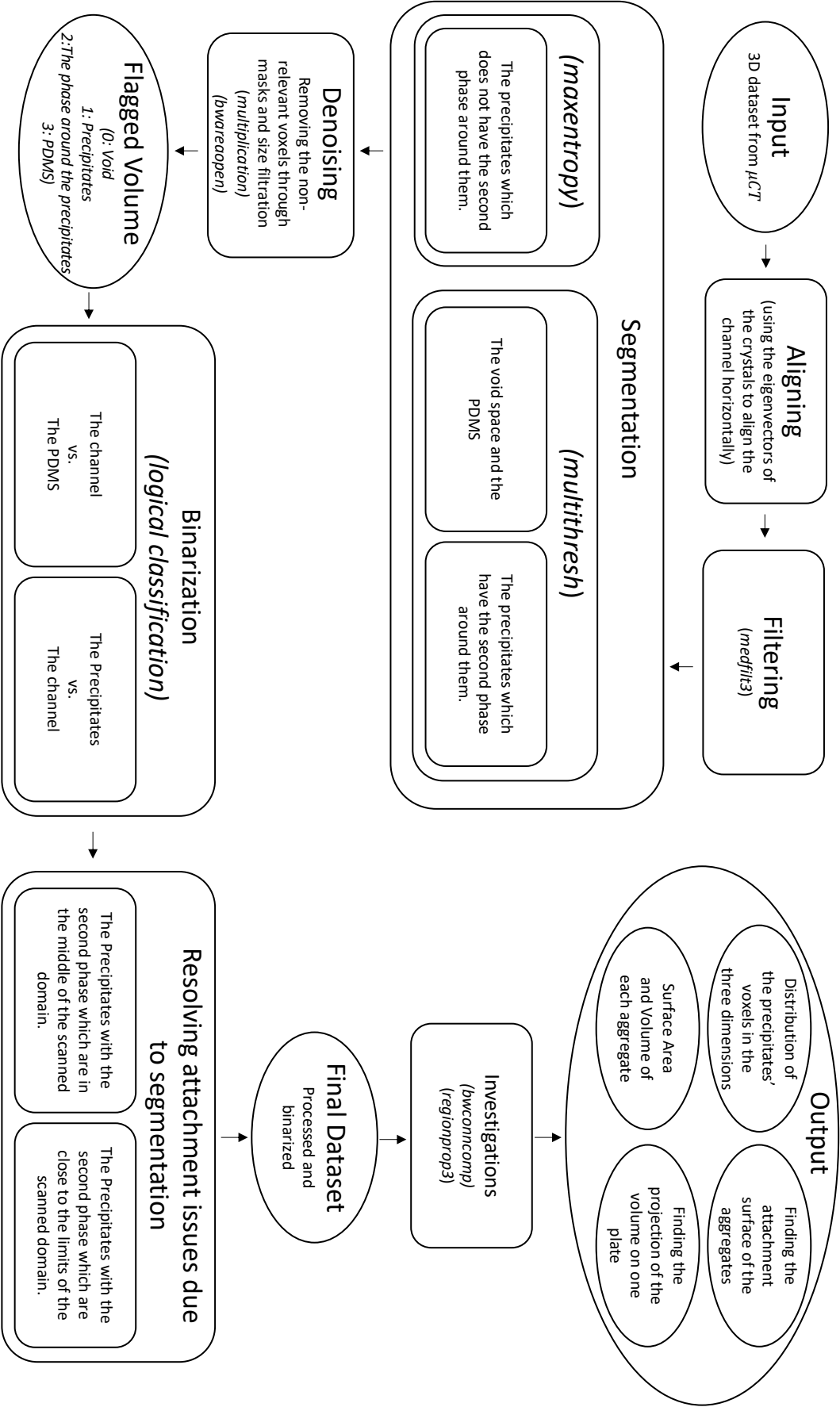
Figure S5. Flow chart of image processing for XRCT images.

Input — 3D dataset from μCT

Aligning (using the eigenvectors of the crystals to align the channel horizontally)

Filtering (*medfilt3*)

Segmentation

(maxentropy) — The precipitates which does not have the second phase around them.

(multithresh) — The void space and the PDMS; The precipitates which have the second phase around them.

Denoising — Removing the non-relevant voxels through masks and size filtration *(multiplication)* *(bwareaopen)*

Flagged Volume (0: Void; 1: Precipitates; 2: The phase around the precipitates; 3: PDMS)

Binarization (logical classification) — The channel vs. The PDMS; The Precipitates vs. The channel

Resolving attachment issues due to segmentation — The Precipitates with the second phase which are in the middle of the scanned domain.; The Precipitates with the second phase which are close to the limits of the scanned domain.

Final Dataset — Processed and binarized

Investigations *(bwconncomp)* *(regionprops3)*

Output — Distribution of the precipitates' voxels in the three dimensions; Surface Area and Volume of each aggregate; Finding the attachment surface of the aggregates; Finding the projection of the volume on one plate

August 6, 2020, 2:08pm